IEEJ Journal of Industry Applications
Vol.6 No.6 pp.449–455 DOI: 10.1541/ieejjia.6.449

Paper

Inter-strand Circulating Current Analysis of End-region Transposed Coil of Power Generator using 3D Multi-layer FEM

Masafumi Fujita[*a)] Member, Takaaki Hirose[*] Member
Takashi Ueda[*] Member, Hiroyuki Ishizuka[*] Member
Masashi Okubo[*] Member, Ken Nagakura[*] Member
Tadashi Tokumasu[*] Senior Member

(Manuscript received Jan. 25, 2017, revised June 12, 2017)

Stator coils of large rotating machines are divided into strands, which are transposed to reduce the inter-strand circulating current loss. Circulating current analysis is required to evaluate the effect of transposition, but full 3D analysis is difficult because of the complicated configuration of the transposed coils. In this paper, magnetic field analysis model using 3D multi-layer finite element method is proposed to calculate the inter-strand circulating current in the stator coil with both transposed and non-transposed parts in the coil end region. Then circulating currents are analyzed considering the magnetic flux in the end region and some transposition patterns are compared.

Keywords: power generator, coil, strand, circulation current, multi-layer FEM, rotating machine

1. Introduction

As the enhancement of the efficiency of power systems has become more important, it is required to evaluate the losses accurately. In the stator windings of large rotating machines such as the power generators, the coil bars are divided into strands to reduce the eddy current loss [(1)] and these strands are usually transposed in the stator core region (active part) [(2)(3)] and sometimes in the coil end region [(4)] to reduce the inter-strand circulating current. To evaluate the circulating current, several works have been performed mainly on the transposition in the active part [(5)–(13)]. The authors also have presented analysis methods which can separately evaluate the causal magnetic fluxes [(10)–(12)]. But as for the transposition in the coil end region, the leakage magnetic flux distributes in the open space and it is not easy to evaluate the flux distribution and the complicated features of the transposed strands. Then, the authors have constructed an analysis model of the circulating current in the coil transposed in the end region with multi-slice 2D finite element method (FEM) [(14)] but the solved problem was on the assumption that the transposition pitch in the coil end region is approximated to be uniform though actual coil end generally has a part without transposition. Furthermore, in the 2D method, the twisted shaped of the strands and the connection part at the most end of the half coil where the strands are shorted cannot be modeled.

As for analysis methods for the twisted object, some methods have been proposed in the field of induction motors, in which rotor bars are skewed. In a widely used multi-slice 2D FEM [(15)–(17)], a skewed rotor is divided in several regions in axial direction and assumed to be step-wise sub-regions. Then, a simplified multi-layer method [(18)], in which each layer has twisted so as to express the skewed rotor slot, has been proposed to consider in-plane eddy current due to the perpendicular flux and the effects of the end-ring of the rotor bar and end windings. In these methods, simple and practical modeling techniques are discussed to enhance the efficiency of the analysis works.

Then, magnetic field analysis model using 3D multi-layer FEM is proposed to calculate the circulating current in the stator bar which includes strands transposed in the coil end region to simulate the detailed structure such as non-uniform transposition configuration or the connection part. Then as an example, circulating current analyses considering with both transposed and non-transposed parts in the coil end regions are performed and the effect of the transposition is discussed for some variations of transposition pattern.

The solved model in this paper is approximated in a step-wise shape which can also be solved with multi-slice 2D FEM. But the proposed method can be expanded to more detailed model with some modification such as twisting the elements and adding the connection part to simulate the returning strand current.

2. Analyzed Machine and Stator Winding

2.1 Analyzed Machine The inter-strand circulating current described here is mainly related to large rotating machines, such as the turbogenerators and the hydrogenerators. In this paper, analyses were performed on a 200MVA class hydrogenerator with frequency of 50 Hz.

2.2 Stator Winding In the generators targeted in this paper, the conductors of the armature windings generally consist of double layers of half coils, which are connected to the corresponding half coils. Figure 1(a) illustrates a typical

a) Correspondence to: Masafumi Fujita. E-mail: masafumi1.fujita@toshiba.co.jp
* Toshiba Corporation
2-4, Suehiro-cho, Tsurumi-ku, Yokohama 230-0045, Japan

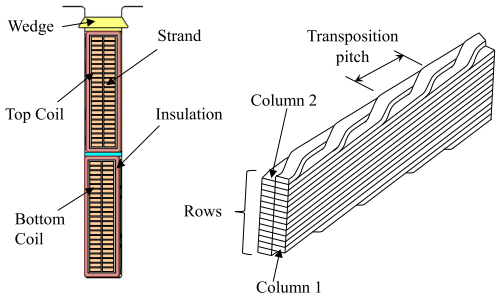

(a) Cross section of coil bar and slot (b) Transposition of strand

Fig. 1. Stator coil of a power generator and strand

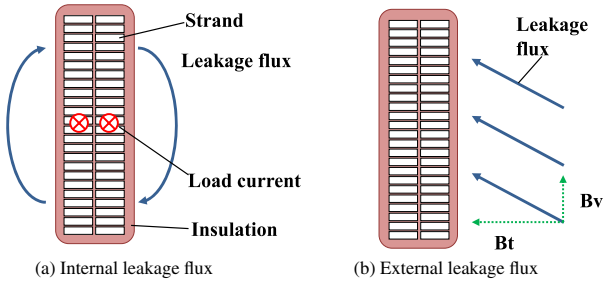

(a) Internal leakage flux (b) External leakage flux

Fig. 2. Coil end leakage flux

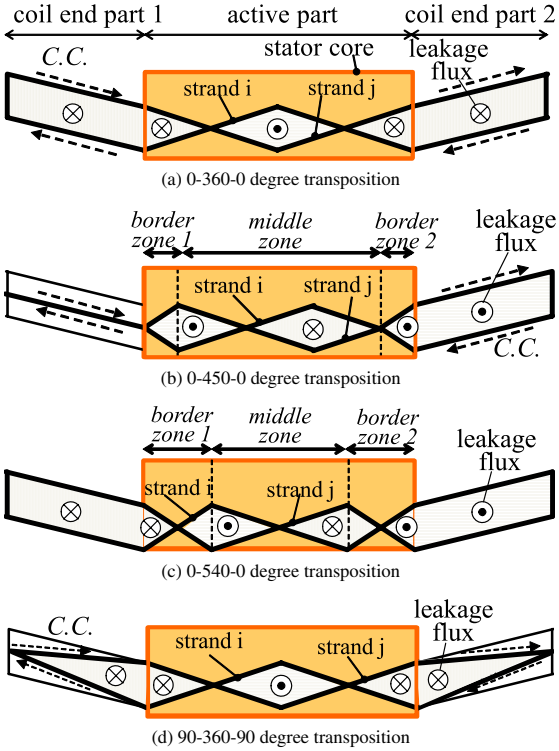

(a) 0-360-0 degree transposition

(b) 0-450-0 degree transposition

(c) 0-540-0 degree transposition

(d) 90-360-90 degree transposition

Fig. 3. Strand transposition variation, where "C.C." denotes the circulating current

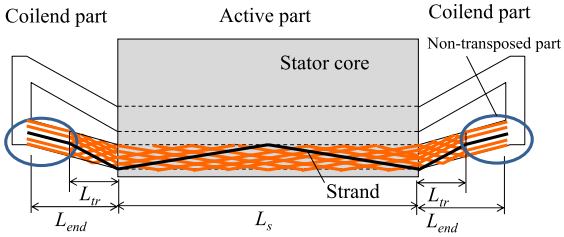

Fig. 4. Strand transposition including coil end regions

cross section of the stator coils. It is composed of layers of mutually insulated conductor strands to reduce eddy current loss. As the strands are shorted at the both ends, electromotive force arises when the induced voltage by the interlinkage flux differs in each strand. Then inter-strand circulating currents are induced which lead to additional losses. In order to eliminate such losses, the strands are commonly transposed as shown in Fig. 1(b).

The conductors are wound and treated by insulating tapes, through which coils are cooled in the indirect cooling type generators. The designers of the generators must be careful to keep the temperature limit of the insulating material not to be damaged. In the analyzed machine, the armature coil is composed of 2 columns and 26 rows of strands.

3. Circulating Current and Strand Transposition

3.1 Circulating Current The loss in the armature winding is classified in the dc resistance loss and ac loss. The ac loss consists of eddy current loss, inter-strand circulating current loss, and inter-circuit circulating current loss in the windings in parallel. The magnetic flux which causes the inter-strand circulating current loss, which is mainly dealt with in this paper, is also divided into slot flux in the core region and coil end flux. Furthermore, the coil end flux is categorized into coil end internal leakage flux (B_i) and coil end external flux. Figure 2 shows schematic diagrams of these fluxes and coil strands. The coil end external flux can be divided into two components of direction, transverse (B_t) and vertical (B_v) to the coil height direction [4]. This classification would be helpful for understanding the circulating current behavior and also for taking measures to reduce the losses.

3.2 Variation of Strand Transposition Figure 3 illustrates the strand transposition diagrams of the stator conductor bar. Figures 3(a) to (c) present the strands which are transposed only in the active part in the core region, namely not transposed in the coil end part. The 360 degree transposition [2] includes the strands which rotate in one cycle in the active part. Similarly, in the 450 degree transposition, the strands rotate in one and a quarter cycle, and in the 540 degree transposition, one and a half cycle [3].

For each transposition configuration, the interlinkage flux in the active part is cancelled when the core is uniform and the strands are transposed as mentioned above. But the voltage induction by the interlinkage flux in the coil end part is doubled in the 360 degree transposition that leads to the circulating current. To improve this, the 450 and 540 degree transposition are aimed to reduce the voltage induction in the coil end part.

As denoted in the caption of the Fig. 4, the transposition configuration is expressed arranging the angle in a coil end part, an active part and another coil end part as "0-360-0", "0-450-0", and "0-540-0" respectively for the 360, 450, and 540 degree transposition in the active part without coil end transposition. As shown in Figs. 3(b) to (c), the transposition pitch in the border zone of the active part is the half of the other part for the "0-450-0" and the "0-540-0" transposition.

Figure 3(d) illustrates an example of the transposition in the coil end parts [4]. The strands are 90 degree transposed in each coil end part as well as 360 degree transposition in the

active part so as to reduce the voltage induction. This type of transposition is expressed as “90-360-90” in this paper.

Figure 4 shows an example of the coil end transposition in the top coil. In this figure, the strands are transposed partly in the coil end region and the transposed area is in the stator core side of the coil end. In this paper, the ratio of the transposed length L_{tr} to the coil end length L_{end} is defined as;

$$R_{tr} = \frac{L_{tr}}{L_{end}} \cdots\cdots (1)$$

The relation between R_{tr} and the circulating current loss is studied in this paper.

4. Analysis Model

4.1 Analysis Model Corresponding to Leakage Flux

As described in the former chapter, the leakage fluxes which produce circulating currents are classified according to their region and their current source. The circulating current can be analyzed separately due to the inducing leakage flux.

The analysis flow is expressed in Fig. 5. First, in the active part, as the coils are surrounded by the magnetic material except at the slot opening, magnetic reluctance to the leakage flux is small and the direction of the leakage flux is mostly restricted to a transverse direction. The radial flux could be neglected especially for the indirectly cooled generators whose slot is much deeper than is wide. Therefore, the circulating current due to the leakage flux in the active part (I_c^a) is calculated by solving network equations on the strand currents [12].

The circulating current due to the leakage flux in the coil end part (I_c^i, I_c^t I_c^v), is calculated separately according to the categorized components in section 3.1. The external flux (B_t, B_v) is calculated by another coil end magnetic field analysis considering the 3D geometry of the coil end region [11].

Then ac analysis is performed using a complex analysis on each categorized flux [10]. The FE analysis model with the coil end region of both sides is analyzed simultaneously with the resistance and the inductance of the strand in the active part.

4.2 2D Method (without Coil End Transposition)

The 2D analysis model considering the coil end flux without coil end transposition is described in (10) and (11). The strands in the coil end region are modeled with 2D meshes and 2 analysis regions represent coil end region 1 and 2 respectively as shown in Fig. 6(a). In each region, a constraint condition is imposed so that the strand current is the same in corresponding strand mesh regions and the flux of all the regions is calculated simultaneously [19][20]. The FE mesh around the coil is depicted in Fig. 6(b). In the figure, the strand number is also indicated.

The governing equation is

$$rot\left(\frac{1}{\mu} rot\boldsymbol{A}\right) = -j\omega\sigma\boldsymbol{A} - \sigma grad\phi \cdots\cdots (2)$$

where $\boldsymbol{A}$ is the magnetic vector potential, ϕ is the electric scalar potential, μ is permeability and σ is conductivity. In the 2D problem, $\boldsymbol{A}$ has only z component and can be written as A_z.

The functional is shown in (3), where Y is the admittance matrix corresponding to the resistance and the inductance of the strand in the active part, β is the element of the cut set matrix which corresponds to the connection between the strands, C is variable corresponding to the strand current, n is the row number of the strands and the suffix k and l corresponding to the strand number. L is the longitudinal length of the analysis region and useful to consider the difference of the coil end length of each end [20]. Note that some of 2D commercial software cannot deal with the analysis regions whose longitudinal lengths are different.

$$\chi = \int \left\{ \frac{(rotA_z)^2}{2\mu} + \frac{j\omega\sigma}{2}\left(A_z - \sum_k \frac{\beta_{kn} C_k}{L}\right)^2 \right\} dS\, L + j\omega \sum_{k,l} Y_{kl} C_k C_l \cdots\cdots (3)$$

Examples of the flux distribution are shown in Fig. 7. Figures 7(b) and 7(c) include 2 analysis regions. As both flux distributions present real part of the complex analysis, which represent the source of magnetic flux. Figure 7(b) illustrates the internal fluxes which originate in the coil current itself. In this model, the total coil current is given and the analysis is done so as the sum of the strand current becomes the total current. Figure 7(c) denotes the end-external fluxes which originate in the flux by the other coils, the rotor coil and the magnetic structures. This analysis deals with the transverse

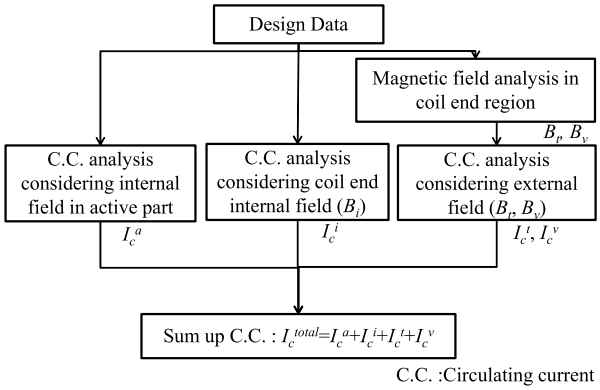

Fig. 5. Analysis flow

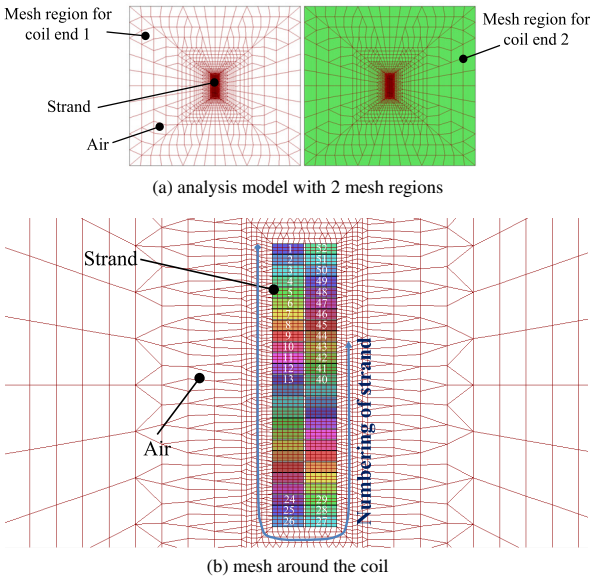

Fig. 6. FE mesh and strand number

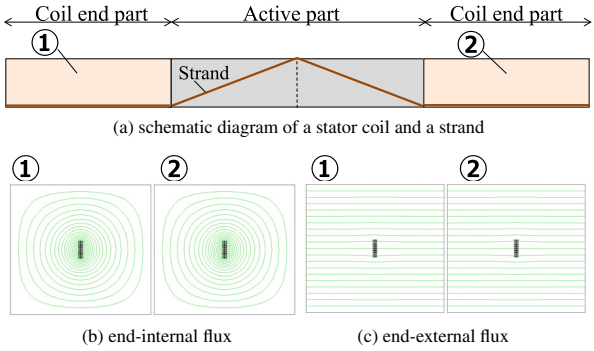

Fig. 7. 2D Circulating current analysis model (without coil end transposition) and examples of flux distribution (real part)

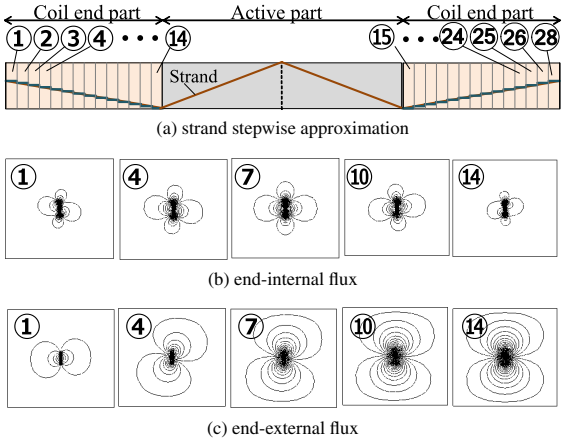

Fig. 8. 2D Circulating current analysis model (with coil end transposition) and examples of flux distribution (imaginary part)

leakage flux and the analysis on the vertical leakage flux is done apart from this analysis. The validation of the analysis has been presented by some of the authors [11] and its summary is described in Appendix.

4.3 2D Multi-slice FEM (with Coil End Transposition) As for the analysis model with coil end transposition, the strands are approximated as step-wise configuration and each step is expressed as a layer of sub-region. When the transposition pitch in the coil end region is uniform and the full length of the coil end strands are transposed, the longitudinal length of the sub-region, L of the equation (3), can be treated as equal [14] and general 2D software is available. In each sub-region, a constraint condition is imposed on the corresponding strand currents similarly to the model of Fig. 6. Figure 8 shows examples of the flux analysis results in the coil end region. In the model of Fig. 8, there are 28 independent analysis regions to express the 13 steps for both coil end regions and the corresponding strands are connected by the external circuit. The shown flux distribution presents the imaginary part, which mainly presents the flux due to the induced current including the circulating current and the eddy current.

4.4 3D Multi-layer FEM To study the problem which cannot be solved with 2D analysis such as the model to express the detail of the twisted strands and the connection part at the most end part of the coil end, 3D multi-layer analysis model has been developed. Here, this model is adapted

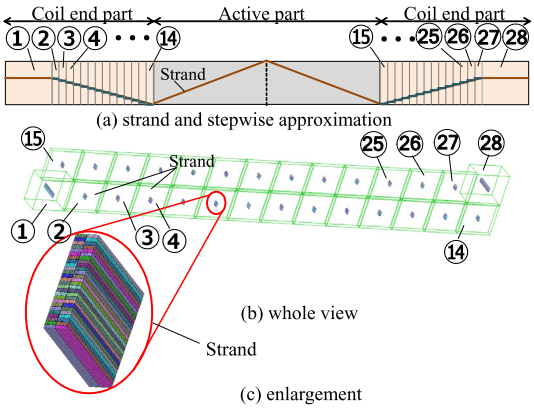

Fig. 9. FE meshes and strand number

to the problem in which there are non-transposed parts in the coil end region.

The governing equation is (2) and the edge element method was applied [21]. The vertical element length of the sub-region is varied corresponding to the longitudinal length of each strand part as shown in Fig. 9.

In Fig. 9, there are 28 independent analysis regions similar to the model of Fig. 8 but the longitudinal length of the region 1 and 28 is larger than the other regions. The corresponding strands are connected with external circuit. In this model, the division number of the element in the longitudinal direction is 1. The external magnetic field is given to each analysis region and the magnetic analysis is performed using the 2-potential method [22].

5. Analysis Results

5.1 Analysis Condition The results solved by the 3D multi-layer FEM is described in this chapter though the problem might be solved by the 2D multi-slice FEM as the strands are approximated with step-wise sub-regions. This is because that this modeling would be suitable to many 3D analysis programs which are available for lots of designers.

For the coil end transposition, non-transposed part is considered. The strands are transposed in the region near the stator core and the ratio of the transposed length to the total coil end length R_{tr} is set to 25, 50, 75 and 100%. In this study, transposition pitch is not restricted though, in the actual design, a minimum transposition pitch is defined due to such as the manufacturing limitations.

5.2 Strand Current The current density contour distribution is displayed in Fig. 10. Though the sub-regions of the analysis model in Fig. 8 are placed side by side, the elements are moved so as to show the longitudinal current distributions. Furthermore, the longitudinal length is multiplied by 0.1 to clarify the distributions. The current due to the external transverse flux and the range of the contour bar is the same in both of the figures. The figures show that the same colored area moves diagonally from the upper left position of the transposed area to the center right position on the front surface of the conductor, which corresponds to the 90 degree coil end transposition. It can be seen that the current density in R_{tr} = 50% (Fig. 10(b)) is lower than that in R_{tr} = 100% (Fig. 10(a)).

Figure 11 shows the strand current distribution, which

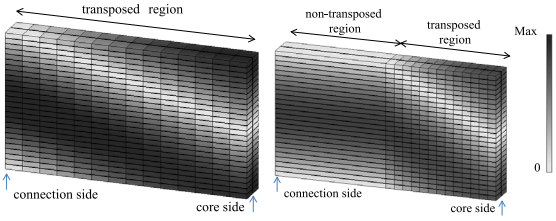

(a) R_{tr} = 100%　　(b) R_{tr} = 50%

Fig. 10. Contours of current density distribution due to the external transverse flux (The longitudinal length is multiplied by 0.1)

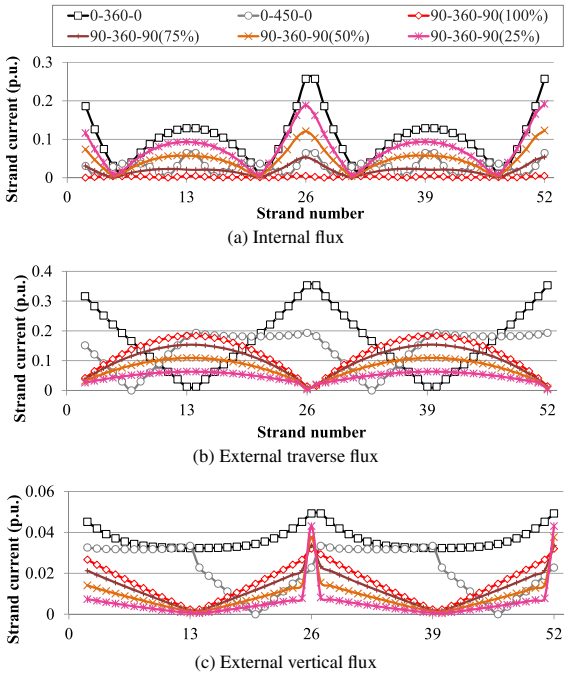

(a) Internal flux

(b) External traverse flux

(c) External vertical flux

Fig. 11. Circulating current distribution in strands for the variation of transposition

depicts the ratio to the averaged load current of each strand. As for the strand number, No.1 denotes the strand in the uppermost and left part and the numbers are defined in the anticlockwise direction as presented in Fig. 6. The circulating current for the "0-540-0" transposition is not presented because it coincides with that for the "0-360-0" for the internal flux and becomes 0 for the external flux. As shown in Fig. 11(a), the "0-450-0" and the "90-360-90" transpositions reduce the circulating current due to the coil end internal flux and the end transposition is the most effective for this flux.

The "0-450-0" and "90-360-90" transpositions partially cancel the voltage induction due to the external flux as shown in Figs. 11(b), (c).

When the transposition ratio R_{tr} becomes larger, the circulating current due to the internal flux becomes smaller as shown in Fig. 11(a). On the other hand, the circulating current due to the external flux becomes large when the ratio increases. This is because that, for the "90-360-90" transposition, the induced voltage in the non-transposed area cancels with each other end part like the "0-540-0" transposition. Therefore if the ratio of transposed length decreases, the area where the voltages are canceled increases.

5.3 Strand Loss Increase Figure 12 shows a

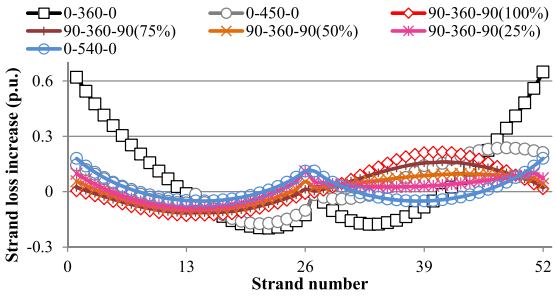

Fig. 12. Distribution of loss increase due to the circulating current for the variations of the transposition

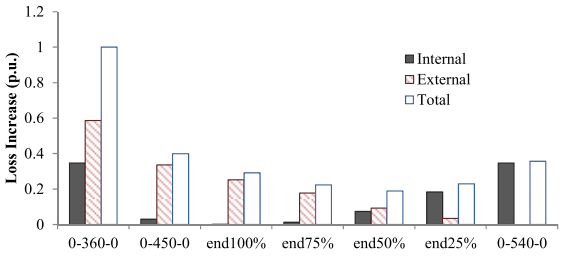

Fig. 13. Transposition variation and loss increase due to circulating current

distribution of loss increase due to the circulating current for the variations of the transposition. The loss increase is the ratio to the dc resistance loss. It is apparent that the loss increase for the "0-360-0" transposition is the largest and the deviation of the strand loss is also large. For the "0-540-0" transposition, the loss and the deviation is the smallest among the transposition variations excluding the coil end transposition. The "0-450-0" and the "90-360-90" transpositions are in the middle of those.

As for the transposition ratio R_{tr}, when it becomes smaller, the loss increase becomes smaller. This inclination is similar to the current due to the external flux because it is dominant on the circulating current.

5.4 Average Coil Loss Increase Figure 13 shows the average loss increase in the coil for the variations of the transposition. The vertical axis is the ratio to the total loss increase of the "0-360-0" transposition. The loss increase due to the internal flux is zero for R_{tr} = 100%, but with the decrease of R_{tr}, the loss due to the internal flux increases. On the other hand, the loss increase due to the external flux decreases along with the percentage. In this case, the total loss increase is the smallest for R_{tr} = 50%.

5.5 Transposition Ratio and Coil End Flux As the total circulating current is the sum of the current due to the internal and external flux, total loss depends on the ratio between the internal and external losses. Figure 14 shows a relation between transposition ratio and the loss increase when the external flux is varied. When the external flux is 2 times the original case, the R_{tr} for minimum loss is 25%. On the other hand, when the external flux becomes smaller, the R_{tr} for minimum loss becomes larger. Namely the optimum percentage varies with the amount of the coil end flux. The R_{tr} should be determined according to the ratio between the internal and the external flux which would change with various design parameters such as coil dimension, coil end length, magnetomotive force ratio between rotor and stator etc.

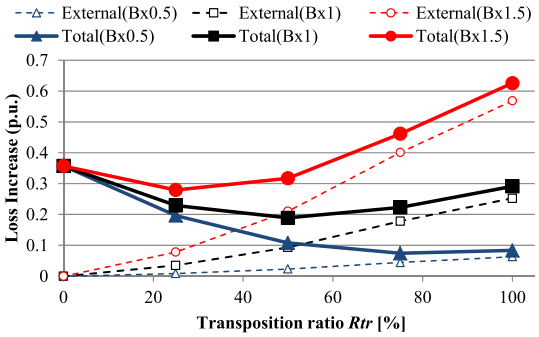

Fig. 14. Transposition ratio and loss increase due to circulating current

6. Conclusion

A circulating current analysis model using 3D multi-layer FEM is proposed and the circulating current losses have been compared on transposition configuration. The loss analysis results considering the magnetic flux in the coil end region have been described.

- By the proposed analysis method, the circulating current in the transposed strands in coil end regions can be evaluated and the loss with respect to each causal magnetic flux can be investigated.

- On the coil end transposition, with the decrease of the longitudinal transposed ratio, the circulating current loss due to the internal flux increases, whereas that due to the external flux decreases.

- On the conditions of the machine dealt with in this paper, the total loss increase is the smallest when the longitudinal transposed ratio is 50% but it depends on the rate of internal and external flux. Therefore the optimum percentage would vary with the amount of the coil end flux.

References

(1) S. Tari, S. Nagano, K. Ito, and T. Kitajima: "Design and operation of water-cooled stator winding for large turbine-driven generator", Toshiba review, Vol.32, No.4, pp.853–858 (1977) (in Japanese)

(2) L. Roebel, Electrical conductor, U.S. patent disclosure 1 144 252 (1915)

(3) W.L. Ringland and L.T. Rosenberg: "A new stator coil transposition for large machines", *Trans. of AIEE*, Vol.78, No.99, pp.743–747 (1959)

(4) H. Sequentz, Herstellung der Wicklungen electrisher Maschinen, Springer-Verlag, Wien (1973) (Japanese Translation by H. Mitsui, M. Matsui and K. Matsunobe, Kaihatsu-sha, 1990, pp.61–64)

(5) K. Takahashi, M. Takahashi, and M. Sato: "Calculation method for strand current distributions in armature winding of turbine Generator", *IEEJ Trans. IA* (in Japanese), Vol.122, No.4, pp.323–329 (2002)

(6) K. Ide, K. Takahashi, K. Hattori, N. Motoi, K. Furukawa, and T. Watanabe: "Practical calculation method of circulating current loss for large turbine generator designs", *IEEJ Trans. IA*, Vol.123, No.5 (2003) (in Japanese)

(7) H. Kometani, H. Yamashita, M. Nakano, and S. Maeda: "Stray load loss analysis for a turbo-generator", IEE Japan, RM-03-114 (2003) (in Japanese)

(8) L. Yanping, B. Xu, Y. Lichao Yang, and W. Lei: "Numerical calculation of circulating current losses in stator transposition bar of large hydro-generator", IET Sci. Meas. Technolo., Vol.9, No.4, pp.485–491 (2015)

(9) B. Xu and L. Yanping: "Circuit Network Model of Stator Transposition Bar in Large Generators and Calculation of Circulating Current", *IEEE Trans. on Industrial Electronics*, Vol.62, No.3, pp.1392–1399 (2015)

(10) T. Tokumasu, Y. Kabata, H. Nakamura, and M. Kakiuchi: "Circulating current analysis of turbine generator stator coil", IEE Japan, RM-03-117 (2003) (in Japanese)

(11) M. Fujita, Y. Kabata, T. Tokumasu, M. Kakiuchi, H. Katayama, and S. Nagano: "Circulating current loss and transposition for stator coil of large turbine generators", IEE Japan, RM-05-145 (2005) (in Japanese)

(12) M. Fujita, Y. Kabata, T. Tokumasu, K. Nagakura, M. Kakiuchi, and S. Nagano: "Circulating currents in stator coils of large turbine generators and loss reduction", *IEEE Trans. on Industry Applications*, Vol.45, No.2, pp.685–693 (2009)

(13) M. Fujita, T. Tokumasu, Y. Kabata, M. Kakiuchi, H. Nakamura, and S. Nagano: "Air-cooled large turbine generator with multiple-pitched ventilation ducts", IEEE International Conference on Electric Machines and Drives (IEMDC), pp.910–917 (2005)

(14) M. Fujita, T. Hirose, T. Ueda, Y. Kabata, H. Ishizuka, M. Okubo, and T. Tokumasu: "Transposition of stator bar strands of generators and inter-strand circulating current loss analysis", International Conference on Power Engineering-15 (ICOPE-15), 1093, Yokohama (Japan) (2015)

(15) K. Yamazaki: "A quasi 3D formulation for analyzing characteristics of induction motors with skewed slots", *IEEE Trans. on Magnetics*, Vol.34, No.5, pp.3624–3627 (1998)

(16) H.C. Lai and D. Rodger: "Comparison of 2D and 3D finite element modelling results of a skewed induction machine", International Conference on Power Electronics, Machines and Drives, pp.365–368 (2002)

(17) A.M. Knight: "Efficient parallel solution of time-stepped multislice eddy-current induction motor models", *IEEE Trans. on Magnetics*, Vol.40, No.2, pp.1282–1285 (2004)

(18) K. Yamada, Y. Takahashi, and K. Fujiwara: "Simplified 3D multilayer modeling for cage induction motors with skewed rotor slots", *IEEE Trans. on Magnetics*, Vol.52, No.3, 8101604 (2016)

(19) T. Nakata, N. Takahashi, and Y. Kawase: "Eddy current analysis of cylindrical parallel conductors including circulating currents", IEE Japan, SA-80-4 (1980) (in Japanese)

(20) T. Tokumasu: "Eddy current analysis by finite element method using circuit theory", IEE Japan, RM-86-38/SA-86-31 (1986) (in Japanese)

(21) A. Kameari: "Calculation of transient 3D eddy current using edge-elements", *IEEE Trans. on Magnetics*, Vol.26, No.2, pp.466–469 (1990)

(22) A. Kameari: "Regularization on ill-posed source terms in FEM computation using two magnetic vector potentials", *IEEE Trans. on Magnetics*, Vol.40, No.2, pp.1310–1313 (2004)

(23) X. Shanchun, W. Zuotan, and L. Rongjien: "A new transposition technique of stator bars of the hydrogenerator", Proceedings of the International Symposium of Salient-Pole Machines (ISSM-93), 10/10-10/12, Wuhan, China, pp.384–389 (1993)

Appendix

Details of the comparison between the analysis result and the measured results are reported in reference (11) by some of the authors. Here, the main results are described.

1. Comparison with The Measurement

1.1 Analyzed Machine The machine studied in this appendix is a 150MVA class, 60 Hz, air cooled turbogenerator, whose stator coils are indirectly cooled with the air flowing in the ventilation ducts arranged in the stator core and the rotor coils are directly cooled with the air flowing through the holes in the coil. As for the stator coil of this machine, two kinds of transposition angle in the active region are settled, 360 degree ("0-360-0") and 350 degree ("0-350-0") respectively. The "0-350-0" transposition includes the strands which rotate in less than one cycle in the active part ("incomplete transposition") [(13)(23)] and intended to reduce the circulating current loss by cancelling the leakage flux in the coil end part [(12)].

1.2 Measurement As the direct measurement of the circulating current loss is not easy, the coil temperature was studied to evaluate the loss distribution. The temperature was measured with the standard resistance temperature detectors (RTDs) installed between the top and bottom coils as illustrated in app. Fig. 1. Operation conditions are no-load (open) and three phase short circuit (short).

1.3 Temperature Analysis The 3D temperature analysis model is shown in app. Fig. 2. The strand losses were calculated by the method described in section 3.2 and given

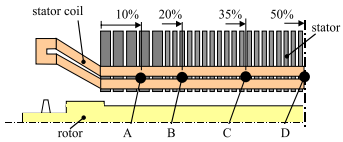

app. Fig. 1. Position of RTDs

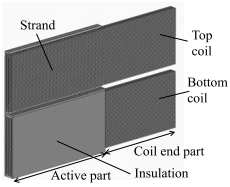

app. Fig. 2. Temperature analysis model

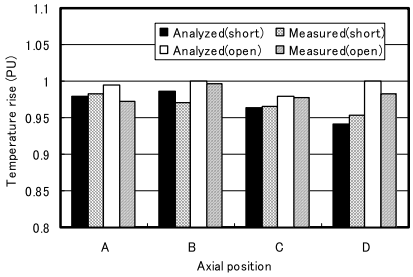

app. Fig. 3. Measured and calculated results of coil temperature rise

in each strand as heat source. The heat transfer boundary condition was calculated with a ventilation analysis considering the ventilation path of the whole generator.

1.4 Comparison of The Results The measured and calculated temperature is shown in app. Fig. 3. The illustrated values are the ratio of the temperature rise in the "0-350-0" transposition coil to that in the "0-360-0" transposition coil. In each location, the measurement and calculation agrees in the range of 2% difference. This result shows the effectiveness of the incomplete transposition and the validity of the analysis.

Masafumi Fujita (Member) received the B.E. and M.E. degrees in electrical engineering from Kyoto University, Kyoto, Japan, in 1989 and 1991, respectively, and the Master of Philosophy degree in electrical engineering from University of Bath, Bath, U.K., in 2004. He joined Toshiba Corporation, Yokohama, Japan, in 1991 and has worked on the design and development of electric machines such as rotating machine based on electromagnetic field analysis. He is a member of the IEEE and the Institute of Electrical Engineers of Japan.

Takaaki Hirose (Member) received the M.E. degrees in electrical and electronics engineering from Nagoya Institute of Technology, Nagoya, Japan, in 2012. He joined Toshiba Corporation, Yokohama, Japan, in 2012 and has worked on the design and development of electric machines such as rotating machine based on electromagnetic field analysis and a member of the Institute of Electrical Engineers of Japan.

Takashi Ueda (Member) received M.E. degree in electrical engineering from University of Miyazaki in 2006 and joined Toshiba Corporation, Japan as a research engineer and works on the computing analysis of electromagnetic field by the finite element method. He is now working in the Business Planning Department of the Thermal & Hydro Power Systems & Services Division and a member of the Institute of Electrical Engineers of Japan.

Hiroaki Ishizuka (Member) received the M.E. degree in electrical engineering from Tokyo Institute of Technology in 1995. He joined Toshiba Corporation, Japan in 1995 and engaged in the design of hydro generators. He is now the specialist of the Generator Engineering Group and a member of the Institute of Electrical Engineers of Japan.

Masashi Okubo (Member) received M.E. degree in electrical engineering from Utsunomiya University in 2001. He joined Toshiba Corporation, Japan in 2001 and engaged in the design of hydro generators. He is now the specialist of the Generator Engineering Group and a member of the Institute of Electrical Engineers of Japan.

Ken Nagakura (Member) received his M.E. degree in electrical engineering from Keio University, Japan in 1998. He joined Toshiba Corporation, Yokohama in 1998, and is working on turbine generator design. He is a member of the Institute of Electrical Engineers of Japan.

Tadashi Tokumasu (Senior Member) received the B.E. degree in physical engineering from the University of Tokyo, Tokyo, Japan, in 1974. He then joined Toshiba Corporation, Yokohama, Japan, as a Research Engineer and works on the computing analysis of electromagnetic field by the finite element method. He is currently the Senior Specialist in the Development and Design Group 2 of Transportation Systems Department. He is a senior member of the Institute of Electrical Engineers of Japan.